Electronic Supplementary Information for:

The role of thryptophan spatial arrangement for antimicrobial-derived, membrane-active peptides adsorption and activity

Irina Schiopu[‡,1], Loredana Mereuta[‡,1], Aurelia Apetrei[1], Yoonkyung Park[2], Kyung-Soo Hahm[3], Tudor Luchian[*,1]

[1] Department of Physics, Laboratory of Molecular Biophysics and Medical Physics, 'Alexandru I. Cuza' University, Blvd. Carol I, No. 11, Iasi 700506, Romania
[2] Research Center for Proteineous Materials, Chosun University, Gwangju, South Korea
[3] BioLeaders Corp., Daejeon, South Korea
[*] Corresponding author, luchian@uaic.ro
[‡] These authors contributed equally to this work

Materials and Methods

Peptide synthesis and purification

Peptides used in this study, termed pep1 (LKRLQKLLSKIWNKW), pep2 (FKRWQKLLSKIWWKN) and pep3 (LKRLQKLLSKIWWKN), were synthesized using 9-fluorenylmethoxycarbonyl (Fmoc) solid-phase methods on Rink amide 4-methyl benzhydrylamine resin (Novabiochem) (0.55 mmol/g) and a Liberty microwave peptide synthesizer (CEM Co. Matthews, NC). To generate N-terminal fluorescently labeled peptides, resin-bound peptides were treated with 20% (v/v) piperidine in dimethylformamide (DMF) to remove the Fmoc protecting group from the N-terminal amino acid. The peptides were cleaved from their respective resins, precipitated with ether, and extracted.[1,2] The crude peptides were purified using reversed-phase preparative HPLC on a Jupiter C_{18} column (250 x 21.2 mm, 15-μm, 300 Å) with an appropriate 0-60% acetonitrile gradient in water containing 0.05% trifluoroacetic acid. The purity of the peptide was then determined by analytical reversed-phase HPLC using a Jupiter Proteo C_{18} column (250 × 4.6 mm, 90 Å, 4 μm). The molecular masses of the peptides were confirmed using matrix-assisted laser desorption ionization mass spectrometry (MALDI II, Kratos Analytical Ins.).[3]

Electrophysiology on artificial lipid membranes

Electrophysiology experiments were carried out in the folded bilayer membranes system obtained with Montal–Mueller technique as described before.[4] A symmetrical lipid bilayer was formed from lipid mixtures containing POPC/DOPG (Avanti Polar Lipids, Inc., USA) dissolved in pentane (85:15 w/w, POPC/DOPG). The bilayer chamber was housed in a Faraday cage, and the electrolyte contained 2 M potassium chloride buffered at a pH value of 7.0 in 10 mM Hepes (Sigma-Aldrich, Germany). Before addition of peptides solution to bilayer chamber, we tested the stability of the membrane in time by subjecting it to positive and negative potentials of up to 170 mV. Once this test completed, and in order to check the functional properties of the membrane, the bilayer was further examined for integrity by adding to the *cis* side of the chamber alamethicin, a well-known active peptide known to form well defined ion channels.   All experiments were performed at a room temperature of $\sim 25^0$C. The insertion of the purified pep1 and pep2 was achieved by adding to the *cis* chamber of the bilayer cuvette, corresponding amounts of the peptide from stock solutions made in distilled water (0.2 mM), to achieve concentrations of 2 μM. All peptides stock solutions were kept at − 20 °C when not used. The particular concentrations used in electrophysiology experiments were chosen based on trial experiments during which we sought to determine the optimal conditions in which the peptides would not destroy the membrane upon insertion, and yet allow to optimally recording of electrical currents induced by it for longer times (> 1 hour). Spontaneous channel insertion was usually obtained within a few minutes while stirring at - (80÷100) mV. We performed at least nine experiments for each peptide, to ensure the reproducibility of the data obtained. Currents from the bilayer chamber were detected with an integrating headstage Axopatch 200 B amplifier (Molecular Devices, USA) or EPC 8 (HEKA, Germany) set to the voltage-clamp mode, via a pair of Ag/AgCl electrodes. Data acquisition of the amplified electrical signals was performed with a NI PCI 6221, 16 bit acquisition board (National Instruments, USA) at a sampling frequency of 30 kHz within the LabVIEW 8.20 environment. Data were than fed into a PC-compatible computer for further numerical analysis and graphing.

Analytical model of peptide insertion in artificial lipid membranes

The accepted view of the general pathways taken by membrane-inserting peptides comprises peptide absorption, interfacial folding, and transmembrane insertion of folded peptides which can be discerned through their center of mass position along the membrane normal and helix tilt angle. For the sake of simplicity, we assume in what follows that only two states exist of peptides orientation with respect to the membrane surface, that is the transmembrane state (TM) whereby the peptide helix is perpendicular to the membrane plane and the interfacial state (IFC) whereby the peptide lies mostly horizontally on the membrane interface (Fig. S1). This is further motivated by the evidence according to which many membrane-active peptides, such as alamethicin, magainin, protegrin, melittin, have been shown to exhibit two distinct states of binding to lipid bilayers.[5,6] While in their interfacial state (IFC), such peptides are believed inactive, since no transmembrane pores were detected,[7] the transmembrane state (TM) of the peptide molecules induce formation of transmembrane pores as demonstrated by neutron diffraction,[8] thus manifesting their lytic function in target cells. In a more detailed description of the so-called peptide-induced toroidal pores in lipid bilayers, it was proposed that the merging of adjacent lipid leaflets through the pore contributes to the pore-forming process, and the edge of the pore is lined by peptides as well as lipid head groups.[9,10]

In this scenario, the ratio of occupancy probabilities of these two states (TM and IFC) at equilibrium, is linked the free energy change associated the transitions between the states according to the equation 1:

$$\frac{P_{TM}}{P_{IFC}} = e^{-\frac{G_{TM} - G_{IFC}}{RT}} \qquad (1)$$

where G_{TM} and G_{IFC} denote the standard molar free energy values associated to the peptide fully inserted into the membrane, and interfacial state of the peptide, respectively, and R, T refer to the gas constant and system temperature (Kelvin degrees).

Given that in addition to their intrinsic dipolar moment, peptides carry net electrical charges, their movement across the membrane in the presence of an applied potential difference is associated to

3

a voltage-dependent part in the free energy change associated the transitions between the interfacial and transmembrane states. Therefore, one can separate the total free energy change of the global transition IFC-TM ($\Delta G_{TM-IFC} = G_{TM} - G_{IFC}$) into a voltage-dependent part ($\Delta G_{TM-IFC}^{el.} = \alpha V$) and voltage independent part ($\Delta G_{TM-IFC}^{non-el.}$) that corresponds to the barriers of interface dislodging and membrane insertion of anchoring residues from the peptides, such as ionizable and aromatic aminoacids. In the voltage-dependent part, we denote by α the molar gating parameter, i.e. the summed product between the each charged atom from the peptide, evaluated for a mole of peptide, and the fractional distance it moves through the membrane during transmembrane insertion. In an oversimplified model, we assume that the electric field across the membrane has contributions only from the applied external potential, and ignore local fields created by charged molecules, or image electric fields. Furthermore, the voltage-dependent part the total free energy change of the peptide global transition IFC-TM, can also contain a supplementary term accounting for the energy stemming from the interaction of its dipole moment with the transmembrane electric field (G_{TM-IFC}^{dipole}), and given as the scalar product of the molar dipole moment of the peptide ($\overrightarrow{M}$) and the transmembrane electric field ($\overrightarrow{E}$) ($G_{TM-IFC}^{dipole} = -\overrightarrow{M} \bullet \overrightarrow{E}$). Considering that in the inserted state, the peptide is oriented parallel to the electric field lines, with the angle between the $\overrightarrow{M}$ and $\overrightarrow{E}$ of zero degrees, and in its adsorbed state it lies parallel to the membrane plane in thus perpendicular to the transmembrane electric field (Fig. S1), the total dipolar free energy change of the peptide global transition IFC-TM equals $\Delta G_{TM-IFC}^{dipole} = -M \dfrac{V}{d}$ (where V is the potential value on the trans side of the membrane, and d its thickness). For simplicity, in this model we disregarded the mechanical contribution to the insertion energy of peptides to lipid membranes, caused by changes in bilayer thickness, modification in the director among adjacent lipid molecules or contribution from the surface tension, stemming from changes in bilayer surface area.[11] Under the influence of an applied potential difference, the activity of peptides which fully insert into the membrane and further oligomerize giving rise to transmembrane pores is responsible for the macroscopic electric behavior of the membrane doped with peptides, manifested as current fluctuations. Considering that the N-terminal of peptides is un-protected, and given the presence of aromatic anchoring

residues at the protected C-terminus, it is fair to assume that during the insertion process, peptides remain anchored to the cis-monolayer interfacial region of the membrane, and the negative potential imposed to the trans-side of the membrane facilitates the rotation of peptides with the positively charged N-terminal head on through the membrane, around their anchored C-terminal. It is important to note that the peptides were engineered as to display similar electric properties, e.g. dipole moment and electric charge. In addition, charged aminoacids were placed in conserved places in the primary structure of peptides. Consequently, it is physically acceptable to assume that the voltage-dependent part of the free energy difference of peptides in the inserted (TM) and interfacial (IFC) states ($\Delta G_{TM-IFC}^{el.}$) is similar. Therefore, the voltage-dependent activity of pep1 and pep2, quantified in this work by the variance of current fluctuations recorded under various holding potentials (see main text), is essentially due to the distinct penalty energy experienced by pep1 and pep2 while dislodging and pulling the anchoring aromatic residues from the cis-monolayer interface through the membrane core, and accommodate them within the bilayer region, as the insertion process proceeds. In other words, the fact that the activity of pep2 is seen to be lower that that of pep1 at any given potential difference, may be interpreted as a lower probability with which pep2 occupies the transmembrane state, and this in turn we propose to be caused mainly by the supplementary energy barrier encountered by pep2 to snorkel into the hydrophobic region of the bilayer due to a the favorable interactions of residues F 1 and W 4 with the to the trans polar head group region of the membrane. Consequently, the curves in Fig. 2, panel c may be fitted with the analytical expression that describes the occupancy probabilities of the TS substate by adsorbed peptides, which can be derived from equation 1 knowing that within the two-states model proposed the sum of occupancy probability of sub-states TS and IFS equals one:

$$P_{TS} = \frac{1}{1 + e^{\frac{\Delta G_{TM-IFC}}{RT}}} = \frac{1}{1 + e^{\frac{\Delta G_{TM-IFC}^{el.} + \Delta G_{TM-IFC}^{non-el.}}{RT}}} = \frac{1}{1 + e^{\frac{\alpha V + \Delta G_{TM-IFC}^{non-el.}}{RT}}} \quad (2)$$

In equation (2), for simplicity and without affecting the overall result – since all peptides possess similar dipolar moments, in the expression of the voltage-dependent part in the free energy change associated the transitions between the interfacial and transmembrane states we disregarded

supplementary term accounting for the energy stemming from the interaction of its dipole moment with the transmembrane electric field. Due to the extremely elevated activity of studied peptides above imposed potentials of -100 mV, which led in many cases to irreversible membrane destabilization, we restricted our experimental points of peptides activity within -50 ÷ -100 mV. By keeping in equation 2 the voltage-dependent part of the difference in free energy between the TM and IFC states (α) invariant for both pep1 and pep2 (*vide supra*), the offset in the voltage-independent part of the free energy change associated to the transition between the two global states of the peptides ($\Delta G_{TM-IFC}^{non-el.}$) quantifies properly the supplementary energy (~ 0.2 kcal/mol) needed to bury the supplementary aromatic residue from pep2 within the bilayer hydrophobic core, namely F 1 and W 4. In a simplistic model, and motivated by energy and geometric arguments, we assume that the most plausible orientation of pep2 in its IFC state is the most stable one, e.g. with F 1, W 4 and W 12 pointing towards the membrane headgroup region of the cis membrane monolayer, and as the insertion progresses, W 12 remains locked at the cis interfacial region (*vide supra*).

Liposomes preparation

Unilamellar vesicles for spectrofluorometric measurements were prepared from a mixture of POPC/DOPG (85:15 w/w) (Avanti Polar Lipids, Inc., USA) and obtained through the hydration method. A defined amount of lipid was dissolved in pure chloroform (Sigma-Aldrich, Germany) and a thin film was formed through high vacuum dehydration of the solvent, which were then hydrated with an aqueous solution of 0.2M KCl buffered with 10mM HEPES at pH 7 to produce a vesicle suspension with a lipid concentration of 1mM. Continuous and vigoros stirring promoted hydration and swallowing of the lipid film thus allowing the formation of multivesicular (MVVs) and multilamellar vesicles (MLVs). The liposome dispersion was subjected to three to four cycles of sonication of 10 min with intervals with an Elmasonic S 80 H sonicator (Germany) in order to obtain a clear lipid solution which indicated the formation of the unilamellar vesicles.

Fluorescence spectroscopy

Interaction between the peptides and unilamellar vesicles present in suspension at concentrations ranging from 20 μM to 300 μM, were studied by monitoring the lipid-induced

spectral blue shift $\Delta\lambda$, corresponding to the change in wavelength of the emission fluorescence signal maximum compared to the lipid-free spectrum as previously described.[12] The spectral blue shift is caused by the less polar environment experienced by the tryptophan residue when adsorbed in the lipid membrane interfacial layer.[13] Peptides were added at a aqueous concentration of 0.5 μM made in prelubricated Costar plastic tubes (Corning, USA) to minimize loss of peptide due to unspecific binding to glass surfaces. The fluorescence measurements were carried out using a FluoroMax-4 (Horiba Jobin Yvon, USA) fluorimeter. The excitation wavelength was set at 280 nm, and seven experiments were recorded for each of the peptides used (i.e., pep1, pep2 and pep3), in the absence and presence of lipid vesicles, during which the emission spectrum was measured between 300 and 450 nm with a 2 nm resolution step.

The values of $\Delta\lambda$ were displayed against the lipid concentration (see Fig. S2, for representative traces), and apparent binding constant (K_a) as well as the maximum fluorescence emission blue shift ($\Delta\lambda_{max}$) were extracted from the non-linear hyperbolic fit according to the equation 3:[14]

$$\Delta\lambda = \Delta\lambda_{max} \frac{K_a[L]}{1 + K_a[L]} \quad (3)$$

where:

$$K_a = \frac{[P]_{membrane}}{[P]_{water}[L]} \quad (4)$$

and $[P]_{membrane}$ refers the molar concentration of the membrane-partitioned peptide and $[P]_{water}$ the molar concentration of the free peptide in the aqueous solution once the partition equilibrium has been reached, and by $[L]$ we denote the molar concentration of vesicle lipids. With the assumption that only the outer leaflet of the lipid vesicles is accessible to peptides, values of [L] were considered half of the total lipid vesicles concentration. Data from at least three experiments were processed in order to estimate mole-fraction free energies of peptides transfer from water to vesicles membrane (kcal/mol), which were calculated from the apparent binding constant (K_a) deduced as described above (equation 4), according to $\Delta G = -RT \ln(K_a[water]) = -RT \ln(K_a 55.5)$.

Calcein leakage experiments

For the calcein leakage experiments we used the same fluorimeter as in the partitioning studies (*vide supra*). Calcein (Sigma-Aldrich, Germany) was dissolved in a saline solution of KCl (50 mM) buffered at pH 7 with 10 mM HEPES, at a concentration of 0.05 M, and was further entrapped in small unilamellar vesicles obtained using the hydration method. Untrapped calcein was separated from the liposomes by gel filtration chromatography on PD-10 desalting columns filled with Sephadex G-25 (GE Healthcare, UK),[15] using an elution solution of 200 mM KCl buffered at pH 7 with 10 mM HEPES. The process of calcein release from liposomes exposed to peptides was recorded by measuring the increase in the fluorescence intensity in the vesicle suspension. The probes were excited at 495 nm and the fluorescence signal determined by the efflux of calcein in the aqueous buffer was recorded at 525 nm, with a 1s time step. The fluorescence intensity corresponding to 100% calcein release was determined by addition of 25 μl of Triton X-100 (1%).

The degree of calcein leakage was subsequently calculated using equation 5:

$$\% \text{ dye leakage} = \frac{(F_x - F_0)100}{(F_{max} - F_0)} \qquad (5)$$

where F_x reprents the fluorescence intensity measured after the addition of the peptide, F_0 is the baseline fluorescence, which was monitored for $\sim$ 30-60 s in the liposome suspension before the addition of the peptide, and F_{max} is the maximum fluorescence intensity measured following the release of all entrapped calcein, upon liposomes lysis by Triton X-100.
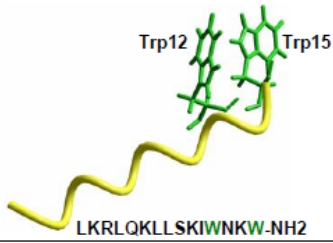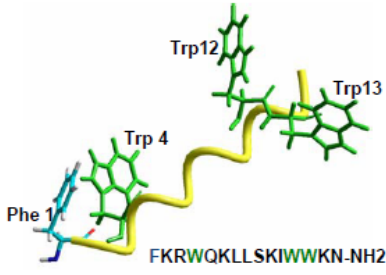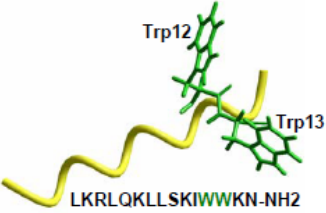
Peptides sequences and idealized secondary structures		$K_a (\mu M^{-1})$ experimental	ΔG interfacial (kcal/mol) experimental	ΔG interfacial (kcal/mol) theoretical	Hydrophobic Moment	Q	Hydrophilicity (Eisenberg scale)
Pep1	Trp12 Trp15 LKRLQKLLSKIWNKW-NH2	0.121	-9.29	-8.52	8.29	6	-0.27
Pep2	Trp12 Trp13 Trp 4 Phe 1 FKRWQKLLSKIWWKN-NH2	0.414	-10.02	-10.38	5.96	6	-0.28
Pep3	Trp12 Trp13 LKRLQKLLSKIWWKN-NH2	0.076	-9.01	-8.52	4.61	6	-0.27

Table S1. Comprehensive view of structural and functional features of the peptides used in this study. When modeled as perfect α-helices, the spatial arrangement of aromatic residues is distinctly seen for pep1, pep2 and pep3. Data in the table present theoretical values of the hydrophobic moments and free energy of transfer for the water to the lipid environment (kcal/mol), as calculated by using the totalizer module of Membrane Protein Explorer (MPEx) (http://blanco.biomol.uci.edu/mpex/), and hydrophilicity, calculated with with HydroMCalc peptide sequence analysis tool, http://www.bbcm.univ.trieste.it/~tossi/HydroCalc/HydroMCalc.html, as well as experimentally derived values for the apparent binding constant (Ka) and free energies of water-lipids transfer ΔG (kcal/mol). Theoretical estimates of hydrophobic moments (μ_H) of peptides (see main text) were made by using the totalizer module of Membrane Protein Explorer (MPEx) (http://blanco.biomol.uci.edu/mpex/).
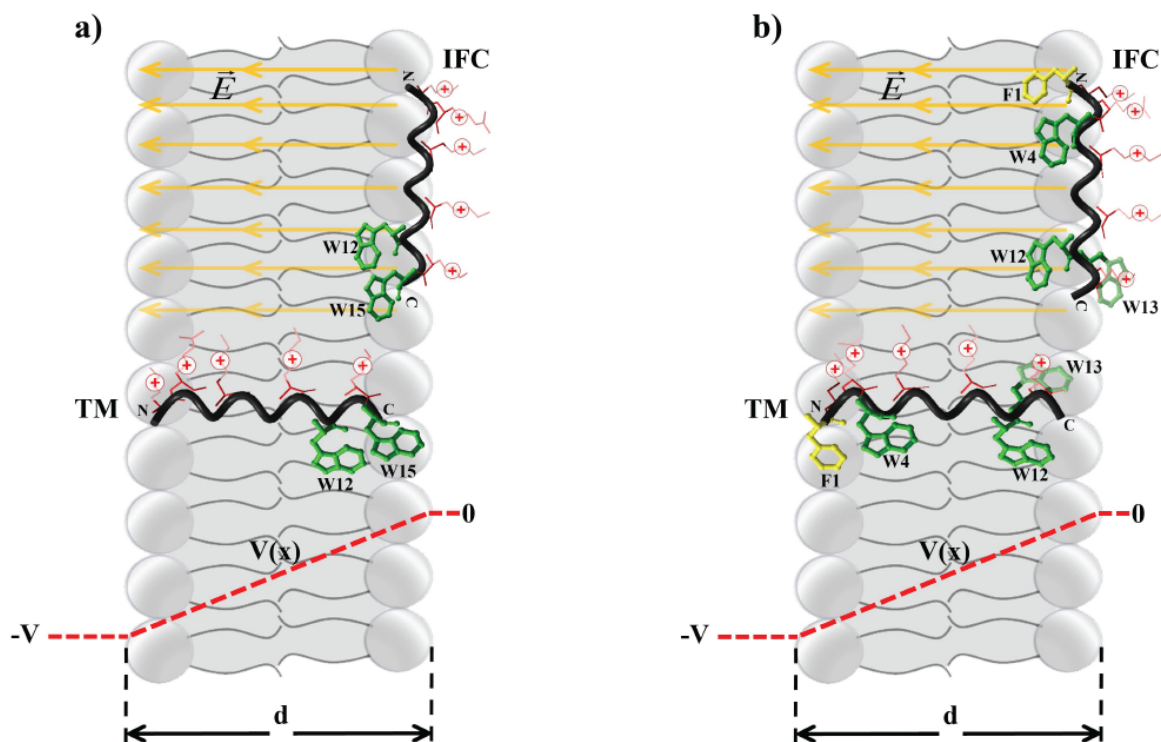
Figure S1. Schematic view of the geometrical orientations assumed by pep1 (panel a) and pep2 (panel b) upon interactions with a model planar lipid membrane. In both cases, peptides are assumed to have been added to the grounded, cis side only (electric potential null) and various negative potentials were imposed on the trans side. If no other charge or dipolar distributions are assumed to contribute to the overall electrostatics, electric field is constant across the membrane interior (yellow lines), and the potential profile varies linearly with the distance within the membrane (the red, dashed line) whose thickness is denoted by 'd'. The probability with which the transmembrane state (TM) is being assumed by either peptide under the applied voltage (-V), depends upon the barriers of interface dislodging and membrane insertion of the peptides, initially adsorbed interfacially on the membrane cis surface (IFC). The Boltzmann fit of voltage-dependent activity of pep1 and pep2 allowed to estimate the barrier to insertion of monomeric peptides into lipid bilayer (i.e., $\Delta G_{TM-IFC}^{non-el.;pep1}$ = -3.5 kcal/mol and $\Delta G_{TM-IFC}^{non-el.;pep2}$ = -3.3 kcal/mol) (see text). The non-linear fit in which the voltage-dependent term was set equal for both pep1 and pep2, resulted in a voltage-independent term of pep2 that is larger that pep1 with ~ 0.2 kcal/mol, which may account partially for the translocation barriers of the extra W 4 and F 1 residues from pep2.
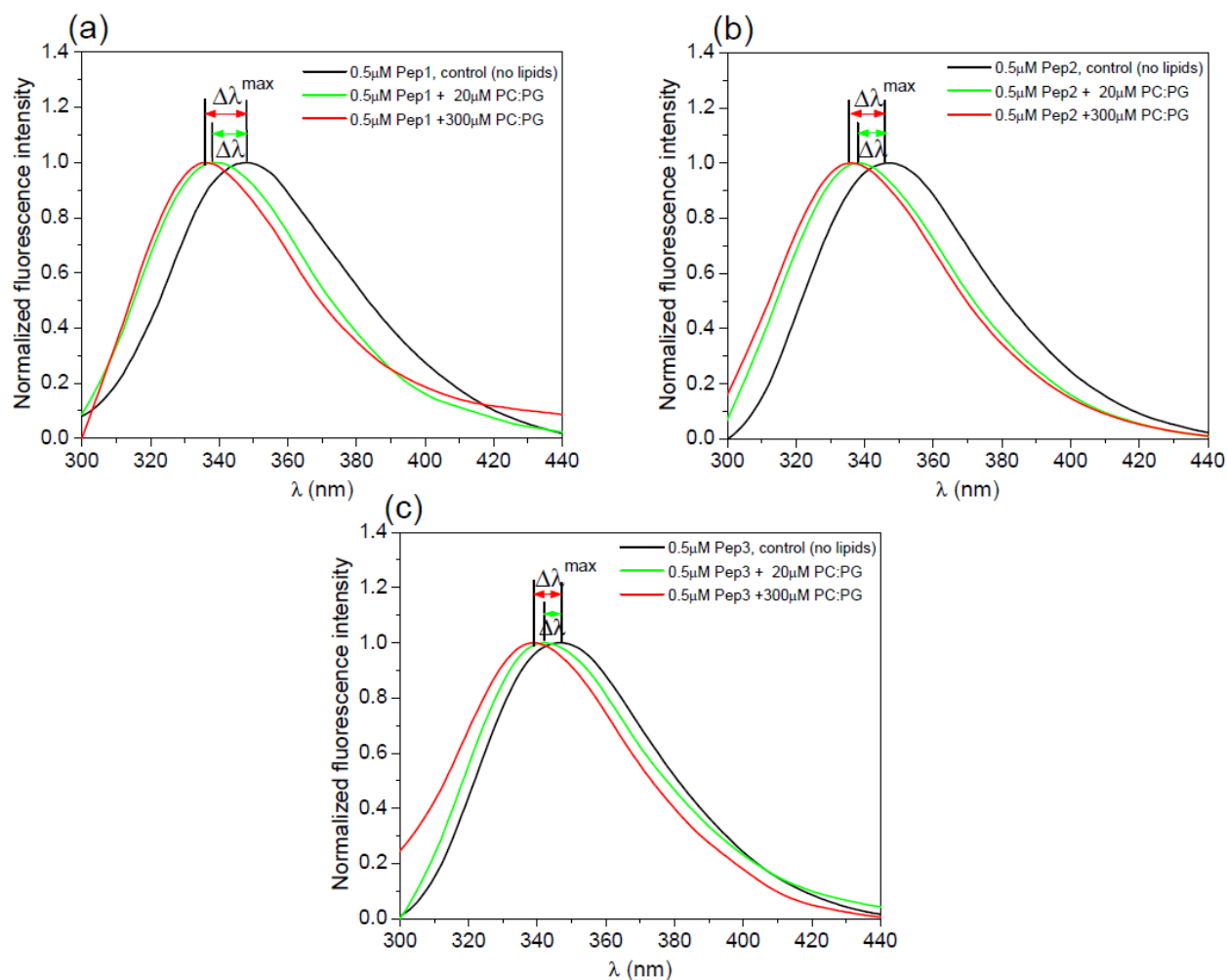
Figure S2. Selected normalized fluorescence traces showing lipid-induced spectral blue shift ($\Delta\lambda$), corresponding to the change in wavelength of the W emission maximum compared to the lipid-free spectrum, to monitor pep1 (panel a), pep2 (panel b) and pep3 (panel c) peptides binding to liposomes. These data were plotted against lipid concentration, to obtain estimates of the maximum fluorescence emission blue shift ($\Delta\lambda_{max}$) and the apparent binding constant (K_a) (see main text).

References

1   J. K. Ghosh, D. Shaool, P. Guillaud, L. Cicéron, D. Mazier, I. Kustanovich, Y. Shai and A. Mor, *J. Biol. Chem.* 1997, **272**, 31609.

2   D. Rapaport and Y. Shai, *J. Biol. Chem.* 1992, **267**, 6502.

3   S. C. Park, M. H. Kim, M. A. Hossain, S. Y. Shin, Y. Kim, L. Stella, J. D. Wade, Y.Park and K. S. Hahm, *Biochim. Biophys. Acta. Biomembr.* 2008, **1778**, 229.

4   A. Asandei, A. Apetrei, Y. Park, K.-S. Hahm and T. Luchian, *Langmuir* 2011, **27**, 19.

5   W. C. Hung, F. Y. Chena and H. W. Huang, *Biochim. Biophys. Acta.* 2000, **1467**, 198.

6   M.-T. Lee, F.-Y. Chen and H. W. Huang, *Biochemistry* 2004, **43**, 3590.

7   L. Yang, T. A. Harroun, T. M. Weiss, L. Ding and H. W. Huang, *Biophys. J.* 2001, **81**, 1475.

8   K. He, S. J. Ludtke, D. L. Worcester and H. W. Huang, *Biochemistry* 1995, **34**, 15614.

9   Y. Shai, *Biochim. Biophys. Acta* 1999, **1462**, 55.

10   S. Qiana, W. Wanga, L. Yangb and H. W. Huang, *PNAS* 2008, **45**, 17379.

11   O. S. Andersen and R. E. Koeppe, *Annu. Rev. Biophys. Biomol. Struct.* 2007, **36**, 107.

12   A. Hawrani, R. A. Howe, T. R. Walsh and C. E. Dempsey, *Biochim. Biophys. Acta* 2010, **1798**, 1254.

13   J. R. Lakowicz, *Kluwer Academic/Plenum, New York, London* 1999.

14   A. S. Ladokhin, M. E. Selsted and S. H. White, *Biophys. J.* 1997, **72**, 794.

15   P. Wessman, A. A. Strömstedt, M. Malmsten and K. Edwards, *Biophys. J.* 2008, **95**, 4324.